

2899-9-T

ENGN
UMR0011

THE UNIVERSITY OF MICHIGAN

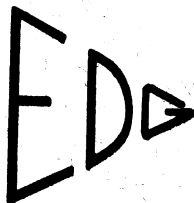
DEPARTMENT OF ELECTRICAL ENGINEERING
ELECTRONIC DEFENSE GROUP

Technical Report No. 96

Some Considerations of Four-Frequency Nonlinear Reactance Circuits

By: D. K. ADAMS

Approved by: H. W



Under Contract With :

CONTRACT NO. DA-36-039 sc-78283,
DEPT. OF ARMY PROJ. NO. 3-99-04-106, PLACED BY:
SIGNAL CORPS ENGINEERING LABORATORIES, FORT MONMOUTH, N. J.

Administered by :

September 1959

THE UNIVERSITY OF MICHIGAN RESEARCH INSTITUTE • ANN ARBOR

ADAMS, D.K.

THE UNIVERSITY OF MICHIGAN RESEARCH INSTITUTE
ANN ARBOR

SOME CONSIDERATIONS OF FOUR-FREQUENCY
NONLINEAR REACTANCE CIRCUITS

Technical Report No. 96

Electronic Defense Group
Department of Electrical Engineering

By: D. K. Adams
=

(David Kendall (1))

Approved by:

Charles B. Sharpe

Charles B. Sharpe

Project 2899

TASK ORDER NO. EDG-4
CONTRACT NO. DA-36-039 sc-78283
SIGNAL CORPS, DEPARTMENT OF THE ARMY
DEPARTMENT OF ARMY PROJECT NO. 3-99-04-106

September 1959

**THE UNIVERSITY OF MICHIGAN
ENGINEERING LIBRARY**

TABLE OF CONTENTS

	Page
LIST OF ILLUSTRATIONS	iv
ACKNOWLEDGEMENT	v
ABSTRACT	vi
1. INTRODUCTION	1
2. GENERAL ENERGY CONSIDERATIONS	3
3. SMALL-SIGNAL THEORY	10
4. CONCLUSION	31
APPENDIX	33
REFERENCES	37
DISTRIBUTION LIST	38

LIST OF ILLUSTRATIONS

Figure	Page
1. General circuit model.	2
2. General characteristics of power conversion gain from ω_1 to ω_2 and ω_3 .	6
3. General characteristics of power conversion gain from ω_2 to ω_1 and ω_3 .	8
4. A small-signal model.	11
5. Representation of a modified external admittance notation.	14
6. A locus of external circuit adjustments for parametric amplification at ω_2 .	22
7. A cascade of upper-sideband up-converters of the type described in Case 2.	28
8. A positive-input-conductance, nonlinear reactance amplifier theoretically capable of unlimited gain.	29

ACKNOWLEDGEMENT

The author wishes to express his appreciation to Professor C. B. Sharpe and to Mr. R. T. Denton for frequent helpful discussions during the course of this research.

ABSTRACT

Several advantages of multiple-frequency nonlinear reactance circuits are described in this paper. In particular, a circuit is considered in which a nonlinear reactance couples four basic frequencies: ω_0 , ω_1 , ω_2 , and ω_3 which are so related that $\omega_2 = \omega_0 + \omega_1$ and $\omega_3 = \omega_0 - \omega_1$. Here, ω_0 is taken to be the power source or pump. It is found to be desirable to allow for the possible presence of the pump harmonic, $2\omega_0$, and individual cases are characterized accordingly as $2\omega_0$ is present or not. The major results are:

(1) Unlimited amplification gain is theoretically possible at frequencies higher than the pump, by reflecting negative input resistance at ω_2 , but without relying on any effects due to the pump harmonic.

(2) Unlimited up- or down-conversion gains between ω_1 and ω_2 are theoretically possible in the presence of the pump harmonic, but without reflecting negative input or output resistance.

(3) Unlimited amplification gain is theoretically possible at frequencies both lower and higher than the pump fundamental, without reflecting negative input resistance.

SOME CONSIDERATIONS OF FOUR-FREQUENCY NONLINEAR REACTANCE CIRCUITS

1. INTRODUCTION

In recent years considerable attention has been given to the unusual properties of nonlinear reactance modulators. The basic attribute of these circuits that has been exploited thus far is frequency-conversion with power gain. Since nonlinear reactance conversion gain can be obtained in the presence of a signal (or reference frequency), a local oscillator (or "pump"), and just one of their sidebands, emphasis to date has been on three-frequency circuits. It has been demonstrated, however, that remarkably different modulator characteristics arise, depending upon the particular choice of sideband (Ref. 1). In the upper-sideband case, the magnitude of conversion gain is limited to the ratio of the output frequency to the input frequency. In the lower-sideband case, arbitrary conversion gain is possible through regenerative action, which reflects negative resistance into both the input and output terminals. Such negative resistance also enhances the input signal; this effect is known as parametric amplification.

In view of the striking differences between the two cases cited, the simultaneous presence of both sidebands causes the anticipation of interesting effects. Several of these effects will be investigated in this paper, and the following major results will be demonstrated:

(1) Parametric amplification is possible at frequencies higher than the pump frequency with no reliance upon effects due to pump harmonics.

(2) In the presence of the first pump harmonic, arbitrary up- or down-conversion gain is possible between the reference frequency and the

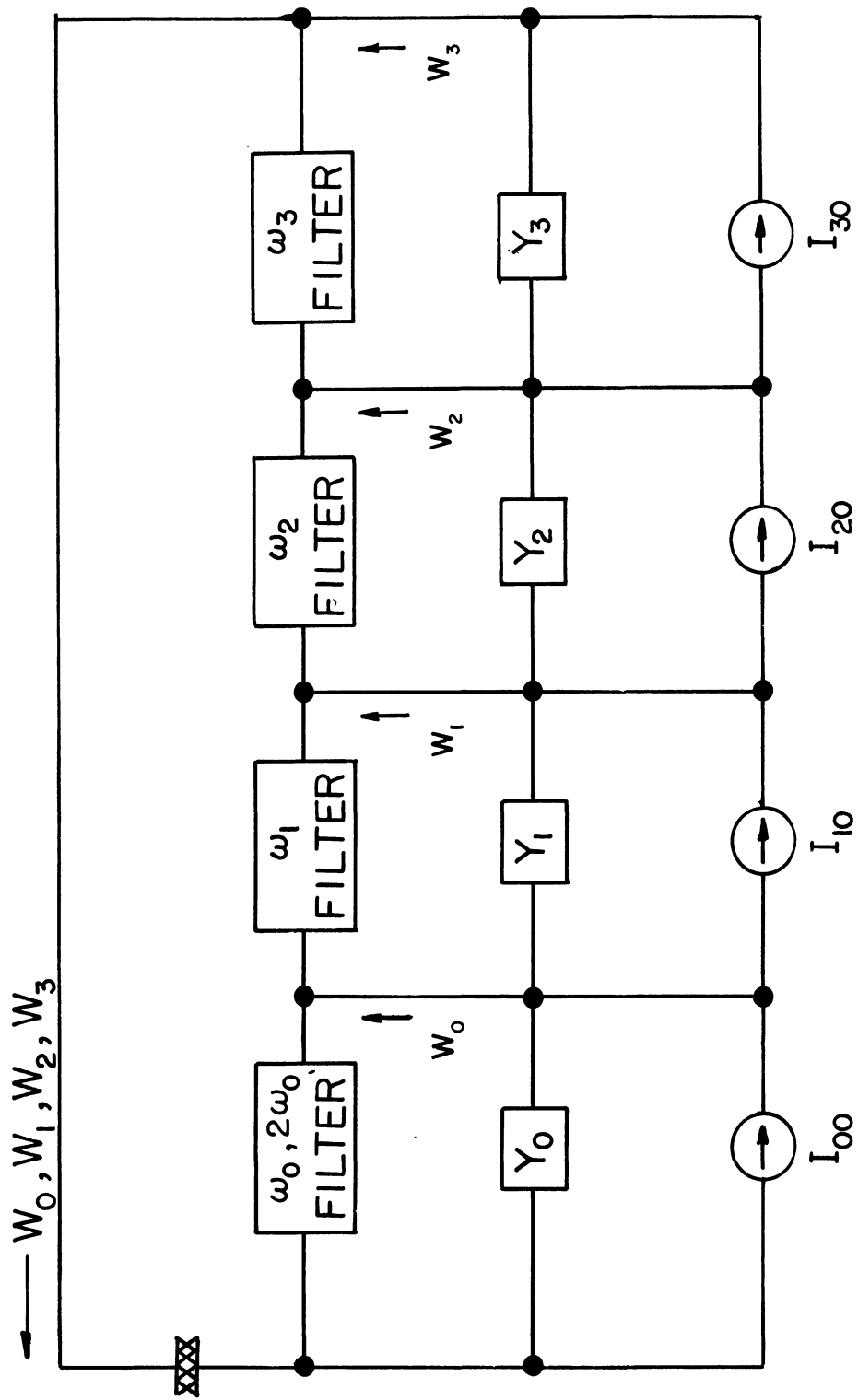


Fig. 1. A general circuit model for the nonlinear reactance problem under discussion.

upper-sideband with no reflection of negative resistance at either frequency. Furthermore, the reflected input and output resistances can be made relatively insensitive to gain.

With nonlinear reactance elements possessing strong nonlinearities and good high-frequency response, the value of the first result lies primarily in its contribution to the general understanding of nonlinear reactance circuits. However, the second result has considerable potential value in spite of its dependence on the presence of the first pump harmonic. As a consequence of statement (2), up- or down-converters of arbitrary gain can be cascaded. In the special case in which an up-converter of the type mentioned above is followed by a similar down-converter, a nonlinear reactance amplifier can be constructed which does not rely on the reflection of negative resistance at the input terminals. Therefore, unlike conventional parametric amplifiers and negative-input-resistance converters, the full potential of this improved converter circuit can be obtained without the use of circulators.

2. GENERAL ENERGY CONSIDERATIONS

The basic problem to be considered in the following analysis is that of a lossless, nonlinear reactance in the presence of signals at ω_0 , ω_1 , and at their upper and lower sidebands: $\omega_2 = \omega_0 + \omega_1$, and $\omega_3 = \omega_0 - \omega_1$. In general, the signal at ω_0 will be considered as the power source or pump and will be assumed to have arbitrarily-large available power. It is practical to allow also for the possible presence of the pump harmonic, $2\omega_0$, since it will be shown to provide valuable effects in some cases. A circuit model for this problem is suggested in Fig. 1, in which a nonlinear capacitor has been chosen to represent the nonlinear

reactive element, and ideal filters have been assumed (1) to short circuit all frequencies except those chosen above, and (2) to allow these frequencies to be coupled only by the nonlinear capacitor. While the assumption of ideal filters seems to be very restricting, the external circuits will ultimately be constrained to be resonant with fairly high Q's. Thus, the ideal filters can eventually be removed without seriously affecting circuit operation.

Although small-signal analysis will be the primary medium employed, a general foundation for the results previously cited is suggested by the general properties of nonlinear reactances. It has been shown by Manley and Rowe (Ref. 1) that the following general statements can be made about lossless, nonlinear reactances in the presence of sinusoidal signals with frequencies from the set $\omega_{mn} = \pm m\omega_0 \pm n\omega_1$, where $m, n = 0, 1, 2, \dots$

$$\sum_{m=0}^{\infty} \sum_{n=-\infty}^{\infty} \frac{mW_{mn}}{\omega_{mn}} = 0 \quad (1a)$$

$$\sum_{n=0}^{\infty} \sum_{m=-\infty}^{\infty} \frac{nW_{mn}}{\omega_{mn}} = 0 \quad (1b)$$

Here, W_{mn} is the average power entering the nonlinear reactance at ω_{mn} , and $W_{mn} = W_{-m, -n}$. The only restrictions on Eqs. 1 are that ω_1/ω_0 be irrational, and that the nonlinear reactive element have a single-valued characteristic. For application to the problem of interest here, Eqs. 1 reduce to

$$\frac{W_0 + W_{20}}{\omega_0} + \frac{W_2}{\omega_2} + \frac{W_3}{\omega_3} = 0 \quad (2a)$$

$$\frac{W_1}{\omega_1} + \frac{W_2}{\omega_2} - \frac{W_3}{\omega_3} = 0 \quad (2b)$$

where the double subscript notation has been dropped, except in the case of average power at the first pump harmonic, W_{20} .

It is important to note that the artifice of restricting the Manley-Rowe relations to a particular set of desired frequencies does not necessarily mean that a predicted result will be generally realizable without the presence of certain of the eliminated frequencies. For example, if the external circuitry reactively terminates a particular frequency, it would be eliminated from Eqs. 1. However, through internal conversion this frequency may be a hidden mechanism behind effects that seem, from Eqs. 1, to be independent of such frequency. This situation arises in this problem in connection with the first pump harmonic. Equation 1a suggests nothing about the relative importance of the pump and its harmonic, and, in fact, falsely suggests that they are interchangeable. Since it is the reactive power of the pump harmonic that is important in this case, W_{20} will be ignored henceforth.

Further study of Eqs. 2 will be divided into two parts.

Consider first the application of signals at ω_1 and ω_0 , with ω_2 and ω_3 seeing passive loads only. Thus, W_2 and W_3 are nonpositive, and Eq. 2b yields the following expressions for up-conversion power gains from ω_1 to ω_2 or ω_3 ,

$$G_{P12} = -\frac{W_2}{W_1} = \frac{\omega_2}{\omega_1} \frac{1}{1 - \frac{W_3 \omega_2}{W_2 \omega_3}} \quad (3a)$$

$$G_{P13} = -\frac{W_3}{W_1} = \frac{\omega_3}{\omega_1} \frac{\frac{W_3 \omega_2}{W_2 \omega_3}}{1 - \frac{W_3 \omega_2}{W_2 \omega_3}} \quad (3b)$$

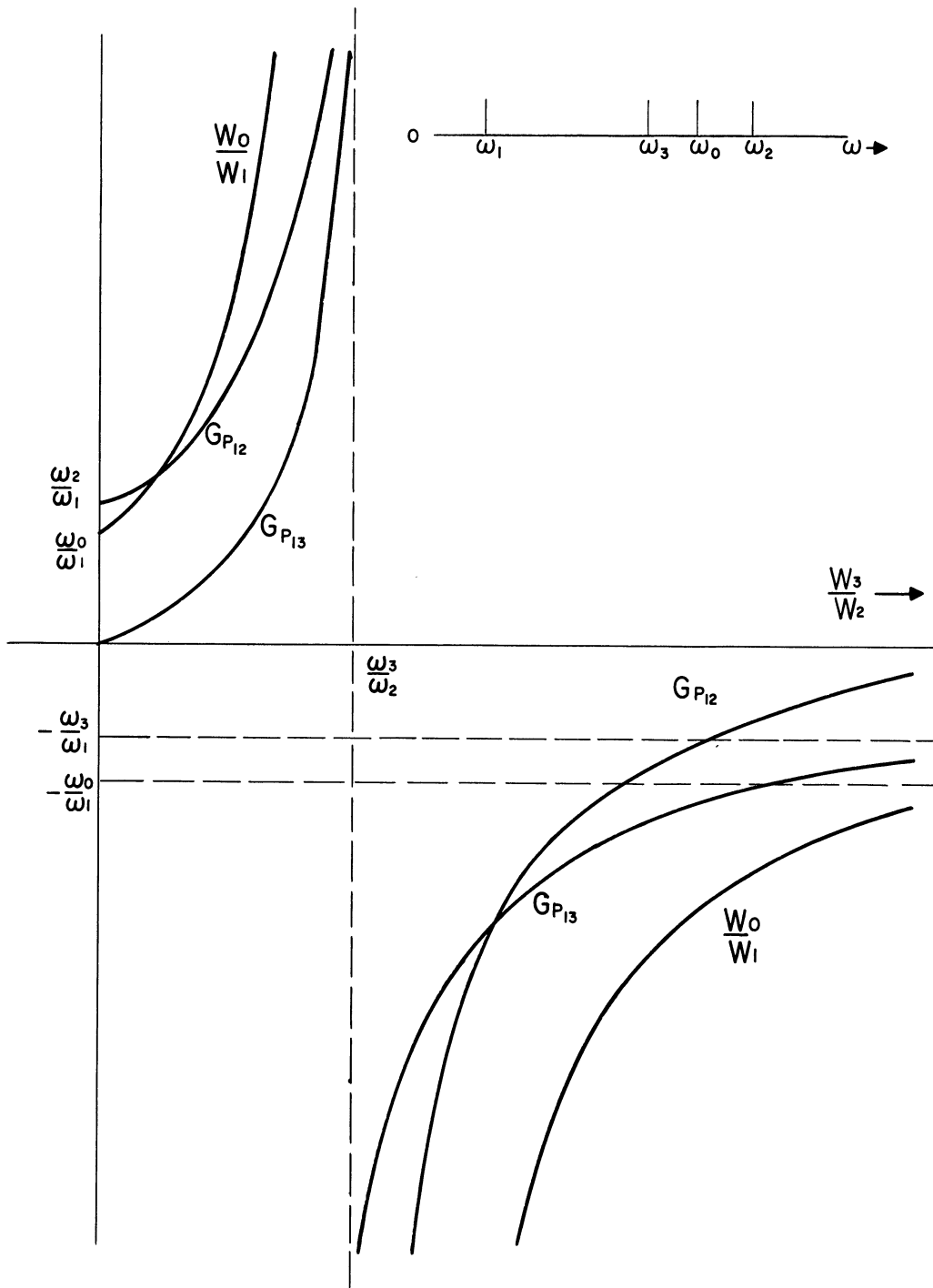


Fig. 2. Sketches of Eqs. (3) showing the regions of positive and negative conversion gains from ω_1 to ω_2 and ω_3 vs. the ratio of output powers at ω_3 and ω_2 . Pump power is applied at ω_0 , and W_0/W_1 is the ratio of pump to signal power.

$$\frac{W_0}{W_1} = \frac{\omega_0}{\omega_1} \frac{1 + \frac{W_3 \omega_2}{W_2 \omega_3}}{1 - \frac{W_3 \omega_2}{W_2 \omega_3}} \quad (3c)$$

To illustrate the remarks to follow, sketches of Eqs. 3 are shown in Fig. 2. In the limit where ω_3 is short circuited ($W_3 = 0$), G_{P12} has the well-known value ω_2/ω_1 . However, G_{P12} increases as $(\omega_2 W_3 / \omega_3 W_2)$ is increased, and arbitrarily-large positive values of G_{P12} can be achieved in the vicinity of $(W_3 \omega_2 / W_2 \omega_3) \lesssim 1$. This suggests that large conversion gain is possible without reflecting negative input conductance at ω_1 . For $(W_3 \omega_2 / W_2 \omega_3) > 1$, G_{P12} and G_{P13} are negative. Hence, this condition defines a general region of potential instability in which parametric amplification is possible at ω_1 . It is important to note that negative conversion gains do not necessarily imply the reflection of negative conductance at the input frequency terminals, although this has been the case in previous nonlinear reactance circuits. Equations 1 would also predict negative conversion gains if the input signal were completely absorbed at one terminal pair, amplified, and then expelled at the same frequency (along with other conversion frequencies) at another terminal pair. The realization of this effect (without using circulators) is one goal of this paper.

The second case of interest is with signals applied at ω_0 and ω_2 , and with only passive loads for ω_1 and ω_3 . In this case Eqs. 2 yield

$$G_{P21} = -\frac{W_1}{W_2} = \frac{\omega_1}{\omega_2} \frac{1}{1 - \frac{W_3 \omega_1}{W_1 \omega_3}} \quad (4a)$$

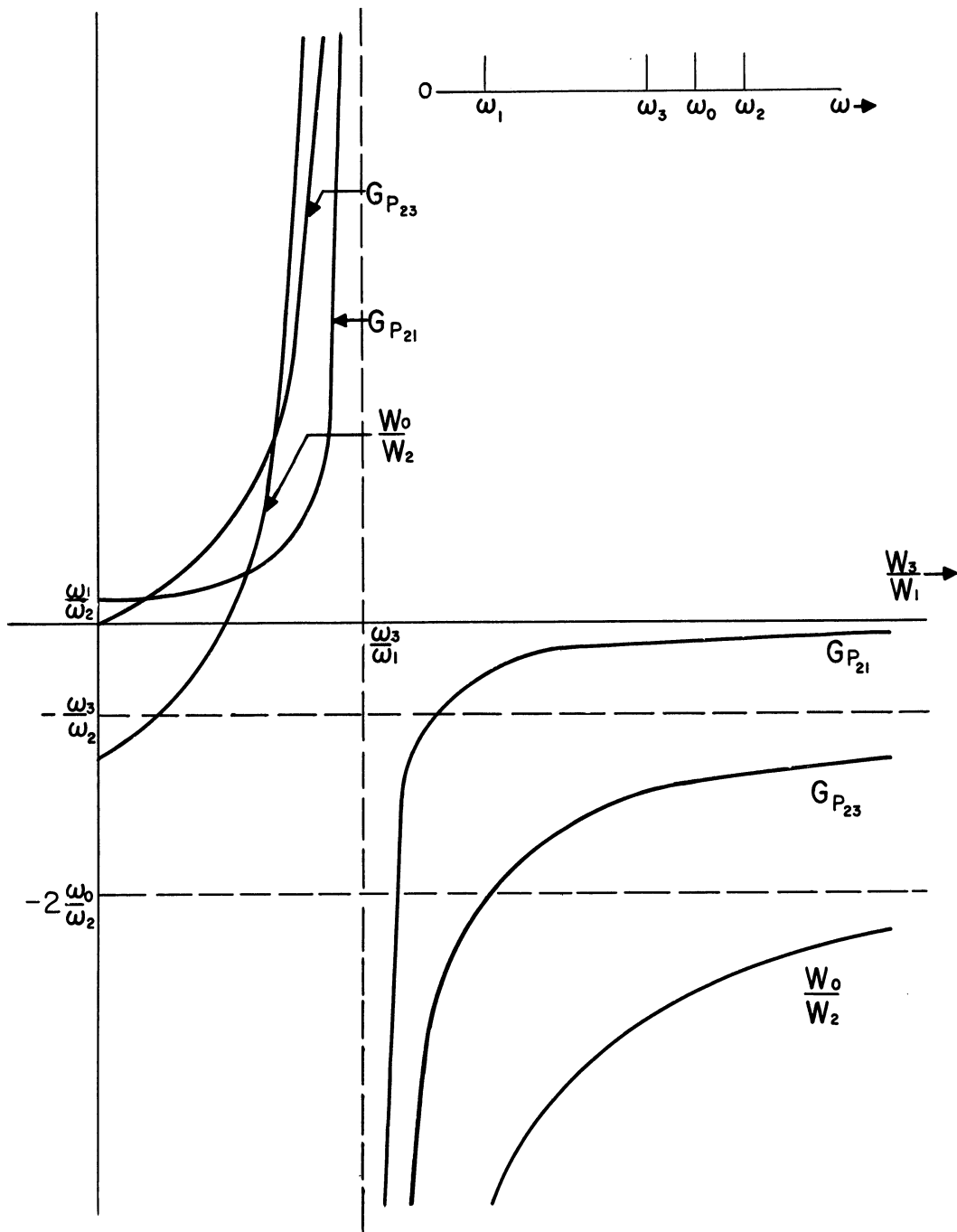


Fig. 3. Sketches of Eqs. (4) showing the regions of positive and negative conversion gains from ω_2 to ω_1 and ω_3 vs. the ratio of output powers at ω_3 and ω_2 . Pump power is applied at ω_0 , and W_0/W_1 is the ratio of pump to signal power.

$$G_{p_{23}} = - \frac{W_3}{W_2} = \frac{\omega_3}{\omega_2} \frac{\frac{W_3 \omega_1}{W_1 \omega_3}}{1 - \frac{W_3 \omega_1}{W_1 \omega_3}} \quad (4b)$$

$$\frac{W_0}{W_2} = \frac{\omega_0}{\omega_2} \frac{2 \frac{W_3 \omega_1}{W_1 \omega_3} - 1}{1 - \frac{W_3 \omega_1}{W_1 \omega_3}} \quad (4c)$$

which are sketched in Fig. 3. For $(W_3 \omega_1 / W_1 \omega_3) < 1/2$, G_{21} and G_{23} are positive, but W_0/W_2 is negative. Therefore, the pump circuit is unstable in this region and the signal at ω_2 will act as the power source. For $(\omega_0/\omega_2) < (W_3 \omega_1 / W_1 \omega_3) < 1$, $G_{p_{21}}$ is greater than unity. Therefore, this is a region of arbitrary down-conversion gain with positive input conductance. For $(W_3 \omega_1 / W_1 \omega_3) > 1$; $G_{p_{21}}$, and W_0/W_2 are negative. Thus, a region of potential instability exists at ω_0 , which suggests that parametric amplification is possible at this frequency.¹

Again it should be noted that Eqs. 1 in no way guarantee that just any nonlinear reactance will yield the results above. For a particular nonlinear reactance, Eqs. 1 may have only the trivial solution, $W_{mn} = 0$. For example, it can be noted from Fig. 3 that parametric amplification at ω_2 is predicted even in the limit where ω_1 is short circuited ($W_1 = 0$).² However, with the nonlinear reactance model employed in small-signal analysis (a model which satisfies the Manley-Rowe equations), it can be

1. The possibility of parametric amplification at ω_2 , using ω_1 and ω_3 as so-called "idler" frequencies, was originally proposed by Hogan et al (Ref. 2). Since this work seems to be based on purely qualitative arguments, parametric amplification at ω_2 will be treated in more detail here. It will be shown that rather unobvious circuit adjustments are required to realize this effect at a small-signal level.
2. This special case has been previously treated through small-signal analysis by Bloom and Chang (Ref. 3).

shown that the pump harmonic ($2\omega_0$) is necessary for parametric amplification at ω_2 , if $W_1 = 0$.

3. SMALL-SIGNAL THEORY

Although the Manley-Rowe equations provide a basis for predicting general properties of nonlinear reactance circuits, they yield no specific information on impedance levels, bandwidth, or the importance of extraneous frequencies. Such information requires further knowledge of the element in question plus mathematical techniques for handling the associated nonlinear circuits. Fortunately, several approximate characterizations of nonlinear elements lend themselves to standard analytical methods. In general, these involve some form of small-signal analysis, the most basic of which neglects responses of the nonlinear element to all signals except the power source and its harmonics. Small signals at all other frequencies then see essentially a periodically varying circuit element at fundamental frequency ω_0 (Refs. 4, 5).

In this section, a nonlinear capacitor will be assumed to be driven by a power source at ω_0 . To employ the small-signal model outlined above, the power source and nonlinear capacitor will be immediately replaced by a periodically varying capacitor for which the following Fourier representation applies.

$$C(t) = \sum_{n=-\infty}^{\infty} C_n e^{jn\omega_0 t} \quad (5)$$

where $C_n = C_{-n}^*$.¹ Now, assuming the external circuitry essentially short-circuits all small-signal frequencies except ω_1 , ω_2 , and ω_3 , the

1. * indicates complex conjugate.

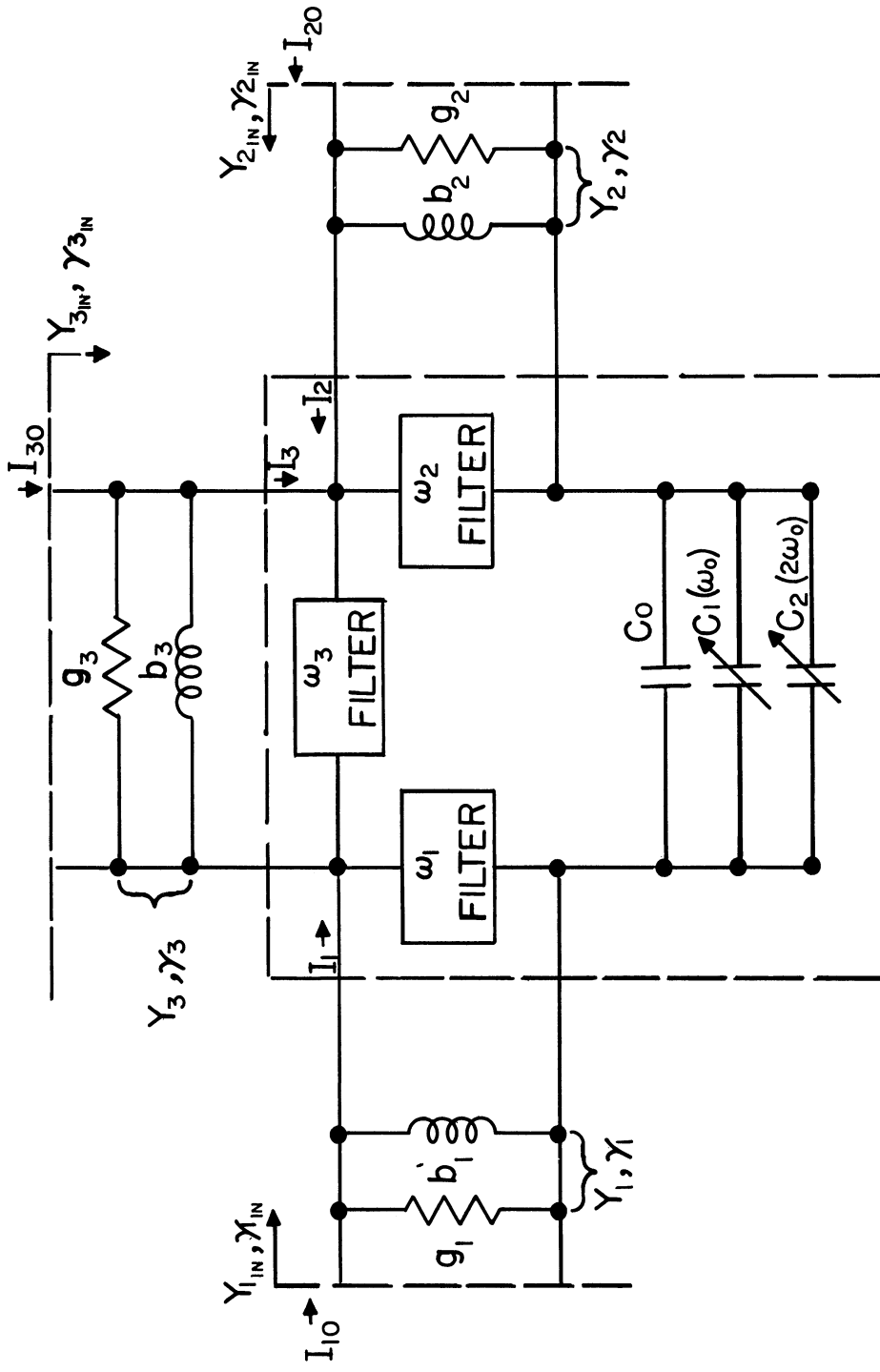


Fig. 4. A small-signal model, based on Eq. (7), for the nonlinear capacitance circuit shown in Fig. 1. Here, γ represents a normalized admittance, according to the definitions in Eq. (12).

small-signal voltage and current across the time-varying capacitor will be given by

$$V(t) = \sum_{n=1}^3 (V_n e^{j\omega_n t} + V_n^* e^{-j\omega_n t}) \quad (6a)$$

$$I(t) = \sum_{n=1}^3 (I_n e^{j\omega_n t} + I_n^* e^{-j\omega_n t}) + (\text{terms representing short circuit currents at other frequencies}) \quad (6b)$$

In Eq. 6b, it is necessary to consider only terms in ω_1 , ω_2 , and ω_3 , since these are the only current components accessible to external terminals.

By combining Eqs. 5 and 6, the following admittance relation is found between the currents and voltages across the time-varying capacitor at each of the small-signal frequencies (Ref. 4).

$$\begin{bmatrix} I_1 \\ I_2 \\ I_3^* \end{bmatrix} = \begin{bmatrix} j\omega_1 C_0 & j\omega_1 C_1^* & j\omega_1 C_1 \\ j\omega_2 C_1 & j\omega_2 C_0 & j\omega_2 C_2 \\ -j\omega_3 C_1^* & -j\omega_3 C_2^* & -j\omega_3 C_0 \end{bmatrix} \begin{bmatrix} V_1 \\ V_2 \\ V_3^* \end{bmatrix} \quad (7)$$

It is important to note, due to the terms in C_2 in Eq. 7, that small-signal effects on ω_1 , ω_2 , and ω_3 will generally include effects of both the pump and its first harmonic. Thus, for a more general formulation of this problem, terms in C_2 will be included.

Equation 7 suggests the linear circuit in Fig. 4 as a small-signal model for this problem. The external admittances present in Fig. 4 are now easily included with Eq. 7 to yield the complete admittance relationship shown below.

$$\begin{bmatrix} I_{10} \\ I_{20} \\ I_{30}^* \end{bmatrix} = \begin{bmatrix} Y_1 + j\omega_1 C_0 & j\omega_1 C_1^* & j\omega_1 C_1 \\ j\omega_2 C_1 & Y_2 + j\omega_2 C_0 & j\omega_2 C_2 \\ -j\omega_3 C_1^* & -j\omega_3 C_2^* & Y_3^* - j\omega_3 C_0 \end{bmatrix} \begin{bmatrix} V_1 \\ V_2 \\ V_3^* \end{bmatrix} \quad (8)$$

In general, two basic phenomena will be investigated with the aid of Eq. 8: (1) power conversion from ω_m to ω_n ; and (2) parametric amplification at ω_m ; where $m, n = 1, 2$ or $2, 1$, respectively. Referring to Fig. 5, if $G_{t_{mn}}$ is the ratio of the output power at ω_n to the available generator power from a source at ω_m , then

$$G_{t_{mn}} = \frac{4g_s (g_{m_{IN}} - g_m)}{|Y_{m_{IN}}|^2} \times G_{p_{mn}} \quad (9)$$

where $Y_{m_{IN}} = g_{m_{IN}} + jb_{m_{IN}}$ is the driving point admittance at terminals (m), g_s is the internal admittance of the input generator, and $G_{p_{mn}}$ is given by Eqs. 3a or 4a. Since $G_{p_{mn}}$ can be alternately expressed by

$$G_{p_{mn}} = \left| \frac{V_n}{V_m} \right|^2 \frac{g_n}{(g_{m_{IN}} - g_m)} \quad (10)$$

Eq. 9 becomes

$$G_{t_{mn}} = \frac{4g_s g_n}{|Y_{m_{IN}}|^2} \left| \frac{V_n}{V_m} \right|^2 \quad (11)$$

Ultimately, conditions will be sought under which $G_{t_{mn}}$ is arbitrarily large. As will be shown shortly, this condition usually arises only when $|Y_{m_{IN}}|$ approaches zero. Since the vanishing of $|Y_{m_{IN}}|$ is also a sufficient condition for parametric amplification at ω_m , first attention will be directed toward this quantity.

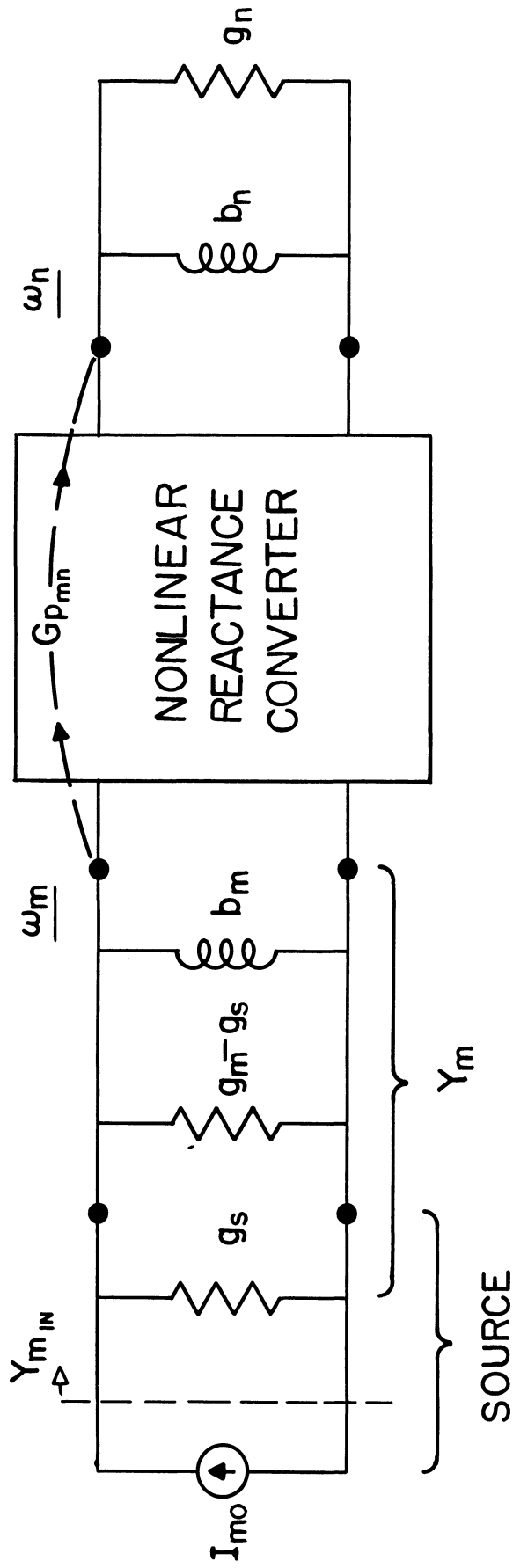


Fig. 5. The modified external admittance notation that is assumed whenever external sources are present, as in the derivation of Eq. (9).

Considerable simplification of the ensuing analysis results if the following normalized admittances are introduced.

$$\gamma_1 = \frac{Y_1 + j\omega_1 C_o}{\omega_1} \left| \frac{C_2}{C_1} \right| ; \quad \gamma_{1_{IN}} = \frac{Y_{1_{IN}}}{\omega_1} \left| \frac{C_2}{C_1} \right| \quad (12a)$$

$$\gamma_2 = \frac{Y_2 + j\omega_2 C_o}{\omega_2 |C_2|} ; \quad \gamma_{2_{IN}} = \frac{Y_{2_{IN}}}{\omega_2 |C_2|} \quad (12b)$$

$$\gamma_3 = \frac{Y_3^* - j\omega_3 C_o}{\omega_3 |C_2|} ; \quad \gamma_{3_{IN}} = \frac{Y_{3_{IN}}^*}{\omega_3 |C_2|} \quad (12c)$$

The notations $\gamma_k = \alpha_k + j\beta_k$ and $\gamma_{k_{IN}} = \alpha_{k_{IN}} + j\beta_{k_{IN}}$ ($k = 1, 2,$ and 3) will also be adopted. The input admittances now take the following normalized forms.

$$\gamma_{1_{IN}} = \gamma_1 + \frac{\gamma_3 - \gamma_2 + 2j\phi}{\gamma_2 \gamma_3 - 1} \quad (13a)$$

$$\gamma_{2_{IN}} = \gamma_2 + \frac{\gamma_3 - \gamma_1 + 2j\phi}{\gamma_1 \gamma_3 - 1} \quad (13b)$$

$$\gamma_{3_{IN}} = \gamma_3 - \frac{\gamma_1 + \gamma_2 - 2j\phi}{\gamma_1 \gamma_2 + 1} \quad (13c)$$

Here,

$$\phi = \frac{\text{Re}(C_1^2 C_2^*)}{|C_1^2 C_2|} \quad (14)$$

and hence is a function of only the relative phases of C_1 and C_2 .

Equations 13 are assumed to apply simultaneously, and express both the normalized input admittances presented to an ideal generator at any

terminal, or the normalized output admittances presented to an ideal voltmeter at any terminal. Therefore, whenever real sources and meters are applied, their internal admittances will be assumed to be lumped with each Y_k or γ_k ($k = 1, 2, 3$), as in Fig. 5.

The form of each of Eqs. 13 readily identifies the physical significance of each term. The first term in each expression for $\gamma_{k\text{IN}}$ is the normalized load admittance at terminals k ($k = 1, 2, 3$), while the second term is the corresponding reflected admittance at terminals k . Inspection of Eqs. 13 reveals that many sets of passive loads exist for which one or more of the $\gamma_{k\text{IN}}$ have negative real parts. This situation will be interpreted as complete instability, and hence Eqs. 13 will be considered physically significant only when the real parts of $\gamma_{1\text{IN}}$, $\gamma_{2\text{IN}}$, and $\gamma_{3\text{IN}}$ are simultaneously positive. In other words, a negative reflected conductance at any terminal pair will be considered useful only when the external conductance at that terminal has the greater magnitude of the two.

Since circuit adjustments are desired that yield large values of $G_{t\text{mn}}$ in Eq. 11, the zeros of $|Y_{m\text{IN}}|$ and the poles of $|V_n / V_m|$ will be of immediate interest. It follows, from the inversion of Eq. 8, that the poles of $|V_n / V_m|$ occur when $|\gamma_m \gamma_3 - 1| = 0$ ($m = 1, 2$). However, by Eqs. 12 and 13, this condition usually yields a pole for $|Y_{m\text{IN}}|$ ($m = 1, 2$). When this is the case, then, the zeros of $|Y_{m\text{IN}}|$ (and hence $|\gamma_{m\text{IN}}|$) are the only infinite gain points. The only exception to this observation occurs when Eqs. 13a and 13b are made independent of γ_3 , which is treated in the section marked Case 2.

Case 1. $|C_2| = 0$

The first application of Eqs. 13 will be to the true four-frequency problem in which all effects of the pump harmonics are assumed negligible. This corresponds to letting $|C_2|$ approach zero, whereupon Eqs. 13 reduce to the following limiting forms:

$$\gamma_{1_{IN}} = \gamma_1 + \frac{\gamma_3 - \gamma_2}{\gamma_2 \gamma_3} \quad (15a)$$

$$\gamma_{2_{IN}} = \gamma_2 + \frac{\gamma_3}{\gamma_1 \gamma_3 - 1} \quad (15b)$$

$$\gamma_{3_{IN}} = \gamma_3 - \frac{\gamma_2}{\gamma_1 \gamma_2 + 1} \quad (15c)$$

Note that $|C_2|$ cancels identically from each of the above expressions. Therefore, it will be required that Eqs. 15, and those to follow in this case, have solutions other than the trivial one, $|C_2| = 0$.

Since Eqs. 15a and 15b cannot be made independent of γ_3 in this case, only arbitrarily small values of $|\gamma_{m_{IN}}|$ ($m = 1$ or 2) will allow unlimited conversion gains from ω_1 to ω_2 , or vice versa. Therefore, when $|C_2| = 0$, the possible advantages of four-frequency circuits over conventional three-frequency circuits are: (1) the reflection of useful negative conductance at ω_1 in the presence of ω_2 , and (2) the reflection of useful negative conductance at ω_2 . Since the latter result is the more novel of the two, in that it provides parametric amplification at a frequency higher than the true pump frequency (i.e., ω_0 , since $|C_2| = 0$), primary consideration will be given to statement (2). This study will

be done under two constraints: (1) $\alpha_{1_{IN}}$, $\alpha_{2_{IN}}$, and $\alpha_{3_{IN}}$ must be positive for stability; and (2) $\beta_{1_{IN}}$, $\beta_{2_{IN}}$, and $\beta_{3_{IN}}$ must be small (preferably zero) at the center operating frequency. The latter condition makes all three terminals nearly resonant, which is desirable as a practical means of eliminating the ideal filters that are tacit to this analysis. Only approximate resonance is required at the external terminals in this case, because it will be shown that some detuning is necessary for parametric amplification at ω_2 to occur.

For purposes of introduction, a special case of four-frequency operation will be described first. One technique for resonating the external terminals is to make $\beta_1 = \beta_2 = \beta_3 = 0$, which means physically that external reactances are chosen to resonate C_0 independently at each terminal. This choice of external reactance, which has been generally satisfactory in conventional three-frequency circuits, is attractive from the practical point of view because it allows circuit adjustments in the "cold" condition (i.e., with the pump turned off). However, this tuning procedure will be shown to be unproductive in this case.

Case 1a. $|C_2| = 0; \beta_1 = \beta_2 = \beta_3 = 0.$

Under these conditions, Eqs. 15 become

$$\alpha_{1_{IN}} = \alpha_1 + \frac{\alpha_3 - \alpha_2}{\alpha_3 \alpha_2} \quad (16a)$$

$$\alpha_{2_{IN}} = \alpha_2 + \frac{\alpha_3}{\alpha_3 \alpha_1 - 1} \quad (16b)$$

$$\alpha_{3\text{IN}} = \alpha_3 - \frac{\alpha_2}{\alpha_1 \alpha_2 + 1} \quad (16c)$$

Inspection of Eqs. 16 shows the condition for stability to be $\alpha_1 \alpha_3 > 1$. Therefore, no useful region of negative reflected conductance exists at ω_2 and the minimum value of $\alpha_{1\text{IN}}$ is limited by circuit stability to $1/\alpha_2$. Thus, parametric amplification at ω_2 is not possible in this case, and the presence of ω_2 limits the gain by parametric amplification at ω_1 . It also follows that little practical improvement of conversion gain results over that possible in conventional three-frequency circuits. Thus, from the point of view of gain, little reward is offered by four-frequency circuits whose external terminals are independently resonant.

It will now be shown, through a more general investigation of Eqs. 15, that the desired negative reflected conductances at ω_1 and ω_2 can be obtained with more arbitrary tuning techniques. These techniques are based on the following general theorems, which pertain to the four-frequency time-varying reactance circuit under consideration here.

Theorem 1: If $|C_2| = 0$ and $\alpha_{1\text{IN}}, \alpha_{2\text{IN}}, \alpha_{3\text{IN}} > 0$, then $\beta_{2\text{IN}} \neq 0$, $\beta_{1\text{IN}} \neq 0$, or $\beta_{3\text{IN}} \neq 0$, is a necessary condition for parametric amplification at ω_2 .

Proof: See Appendix.

Theorem 2: If $|C_2| = 0$, the necessary and sufficient conditions for $\alpha_{1\text{IN}}, \alpha_{2\text{IN}}, \alpha_{3\text{IN}} > 0$ and $\beta_{1\text{IN}} = \beta_{3\text{IN}} = 0$ (i.e., a stable circuit with resonant terminals at ω_1 and ω_3) are:

$$\beta_3 = 0 \quad (17a)$$

$$\beta_2 = \beta_1 |\gamma_2|^2 \quad (17b)$$

$$\alpha_1 - \frac{1}{\alpha_3} > \frac{-\alpha_2}{|\gamma_2|^2} \cdot \left[\text{lesser of } \left(1, \frac{\beta_2^2}{\alpha_2} \right) \right] \quad (17c)$$

Proof: See Appendix.

It should be noted that Theorem 2 can be applied to conventional parametric amplifiers in the case where the upper sideband (ω_2) is not completely shorted, but where the pump harmonic is suppressed. In this case, Eq. 17b indicates that "cold" tuning is not sufficient and some retuning must accompany changes in pump level.

In view of Theorem 1, parametric amplification at ω_2 will be approached by only requiring the terminals at ω_2 to be resonant ($\beta_{2_{IN}} = 0$), for then $|Y_{2_{IN}}|$ approaches zero as $\alpha_{2_{IN}}$ approaches zero. The additional assumption that $\beta_3 = 0$ will be shown below to lead to useful solutions.

Case 1b: $|C_2| = 0$; $\beta_3 = 0$; $\beta_1 \neq 0$, $\beta_2 \neq 0$. Equations 15 now yield

$$\frac{-\alpha_2}{|\gamma_2|^2} < \alpha_1 - \frac{1}{\alpha_3} < 0 \quad (18)$$

as the condition for: (1) stability at ω_1 and ω_3^1 , and (2) the reflection of negative conductance at ω_2 . If Eq. 18 is satisfied, the condition for resonance at ω_2 then becomes:

$$\left(\alpha_1 - \frac{1}{\alpha_3} \right)^2 + \left(\beta_1 - \frac{1}{2\beta_2} \right)^2 = \left(\frac{1}{2\beta_2} \right)^2 \quad (19)$$

If Eq. 19 is satisfied, the condition for stability at ω_2 is

$$\beta_2 < \beta_1 |\gamma_2|^2 \quad (20)$$

1. If $\beta_3 = 0$, it can be shown, as α_3 decreases, that ω_3 never becomes unstable before ω_1 becomes unstable. Thus Eq. 18 only explicitly defines the region of stability at ω_1 .

These conditions are made clearer in Fig. 6, which is a plot of Eq. 19 for $\alpha_1\alpha_3 < 1$. Here, β_1 is considered to be the independent variable determining the magnitude of negative reflected conductance at ω_2 . Point A is the threshold of parametric amplification at ω_2 , point B marks the threshold of circuit instability at ω_1 (Eq. 18), while infinite gain at ω_2 corresponds to the point C (Eq. 20). Therefore, useful parametric amplification at ω_2 may be limited to the finite gains corresponding to the range between points A and B on the tuning curve in Fig. 6. This limitation on gain can be overcome by choosing $\alpha_2^2 = \beta_2^2$, which makes the points B and C coincide. In this case, the negative conductances reflected at both ω_1 and ω_2 allow arbitrary gain at either frequency. It can be shown that a similar result is possible if the terminals at ω_1 are constrained to be resonant while those at ω_2 are detuned.

Thus, in the notation of Fig. 4, sufficient conditions for arbitrary gain by parametric amplification at ω_2 (and at ω_1), with $|C_2| = 0$, are:

$$b_3 + \omega_3 C_0 = 0 \quad (21a)$$

$$g_2^2 = b_2^2 \quad (21b)$$

$$\frac{1}{2} < \frac{b_1 b_2}{\omega_1 \omega_2 |C_1|^2} < 1 \quad (21c)$$

$$\left[\frac{g_1}{\omega_1 C_1^2} - \frac{\omega_3}{g_3} \right]^2 + \left[\frac{b_1}{\omega_1 C_1^2} - \frac{\omega_2}{2b_2} \right]^2 = \left[\frac{\omega_2}{2b_2} \right]^2 \quad (21d)$$

It is important to note that conditions 20 or 21c satisfy Theorem 2 only at the point of infinite gain ($\beta_1\beta_2 = \frac{1}{2}$). Thus, as previously mentioned, the terminals at ω_1 and ω_3 are not resonant in this case and suffer detuning at center frequency by an amount given by:

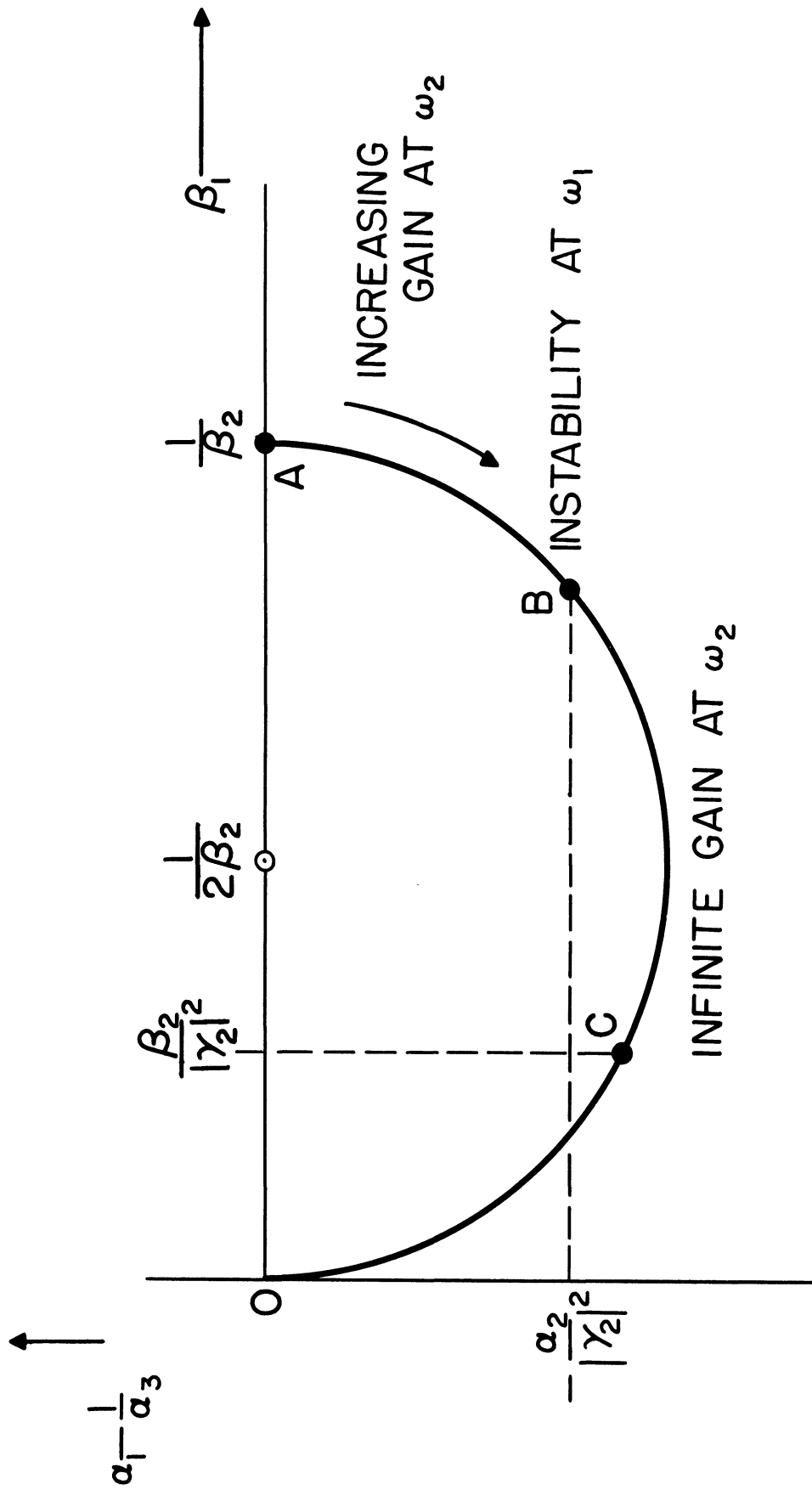


Fig. 6. The locus of external circuit adjustments for tuning and parametric amplification at ω_2 , as described in Case 1b.

$$b_{1_{IN}} = b_1 - \frac{\omega_1 \omega_2 |C_1|^2}{2b_2} \quad (22a)$$

$$b_{3_{IN}} = \frac{2b_2 \omega_1 \omega_3 |C_1|^2 (2b_1 b_2 - \omega_1 \omega_2 |C_1|^2)}{(2g_1 b_2 + \omega_1 \omega_2 |C_1|^2)^2 + (2b_1 b_2 - \omega_1 \omega_2 |C_1|^2)^2} \quad (22b)$$

Equations 22 indicate that the amount of detuning at ω_1 and ω_3 is very small when the gains at ω_2 (or at ω_1) are large.

Therefore, if $|C_2| = 0$, the operation described in Fig. 6 (with points B and C coincident) allows: (1) arbitrary gain by parametric amplification at either ω_1 or ω_2 ; and (2) arbitrary up- or down-conversion gain between ω_1 and ω_2 . Both these effects arise through the reflection of negative conductance at the input terminals and are accompanied by some detuning of the terminals either at ω_1 or ω_2 .

Case 2: $|C_2| \neq 0$

It has been shown previously that the design of idealized, three- or four-frequency, nonlinear reactance converters for large, small-signal, conversion gains (i.e., small-signal gains considerably greater than the ratio of output frequency to input frequency) must invariably rely on the reflection of negative resistance at the input terminals. Consequently, such devices frequently employ circulators as auxiliary equipment in an effort to reduce noise figures and to increase gain-bandwidth products. It will now be shown, when $|C_2| \neq 0$, that arbitrarily large conversion gains are possible between ω_1 and ω_2 without reflecting negative resistance at either frequency. Thus, the importance of circulators in high-gain, nonlinear reactance converters can be eliminated.

The technique for achieving the result cited above is to choose external circuit components that allow $|V_n / V_m|$ to be arbitrarily large (see Eq. 11) without producing a similar effect on Y_{mIN} ($m, n = 1, 2$ or $2, 1$, respectively). It has been previously remarked that this condition can be achieved by making Eqs. 13a and 13b independent of γ_3 , which can be accomplished only if

$$\gamma_1 = \gamma_2 = \sqrt{1-\phi^2} + j\phi \quad (23)$$

Obviously, only the positive square root is permitted here, as will be the case henceforth unless (+) signs are specifically indicated. Substitution of Eq. 23 into Eqs. 13a and 13b yields

$$\gamma_{1IN} = \gamma_{2IN} = 2\sqrt{1-\phi^2} \quad (24a)$$

Thus, when Eq. 23 is satisfied, the terminals at ω_1 and ω_2 are conjugately matched for all γ_3 . Similarly, Eq. 13c reduces to

$$\gamma_{3IN} = \gamma_3 - \sqrt{1-\phi^2} + j\phi \quad (24b)$$

which indicates that a constant negative conductance is reflected at ω_3 . Consequently, $\alpha_3 > \sqrt{1-\phi^2}$ must be required for stability.

Although γ_{mIN} ($m = 1, 2$) has been made independent of γ_3 , it can be shown that $G_{t_{mn}}$ still has a useful pole as a function of γ_3 . By solving Eq. 8 for $|V_n / V_m|$, and using Eqs. 12, Eq. 11 yields the following gain expressions:

$$G_{t_{12}} = \frac{\omega_2}{\omega_1} \left[\frac{(\alpha_3 \pm \sqrt{1-\phi^2})^2 + (\beta_3 + \phi)^2}{(\alpha_3 - \sqrt{1-\phi^2})^2 + (\beta_3 + \phi)^2} \right] \quad (25a)$$

$$G_{t_{21}} = \frac{\omega_1}{\omega_2} \left[\frac{(\alpha_3 \mp \sqrt{1-\phi^2})^2 + (\beta_3 + \phi)^2}{(\alpha_3 - \sqrt{1-\phi^2})^2 + (\beta_3 + \phi)^2} \right] \quad (25b)$$

Here, the (+) signs arise because ϕ specifies only the magnitude of the relative phase angle between C_1 and C_2 and not its sign. In each of Eqs.

25 the upper sign corresponds to $\text{Im}(C_1^2 C_2^*) > 0$ while the lower sign corresponds to $\text{Im}(C_1^2 C_2^*) < 0$. Thus, for a given value of ϕ , there are two possible up-conversion gains and two possible down-conversion gains.

In the case of negative square roots, both $G_{t_{12}}$ and $G_{t_{21}}$ reduce to the ratio of output to input frequency, independently of γ_3 ; while with the positive square roots both $G_{t_{12}}$ and $G_{t_{21}}$ become arbitrarily large as γ_3 approaches the value $\sqrt{1-\phi^2} + j\phi$ (assuming, for stability, that it does so with $\alpha_3 > \sqrt{1-\phi^2}$). Within a single converter stage, however, Eqs. 25 can not be simultaneously satisfied with positive square roots, which yields the useful result that each converter stage is semi-directional. The directivity is dependent on both the forward gain and the relative magnitudes of the frequencies employed.

Perhaps the most practical operating condition is with the terminals at ω_3 resonant (i.e., $\beta_3 = -\phi$), whereupon Eqs. 25 reduce to:

$$G_{t_{12}} = \frac{\omega_2}{\omega_1} \left[\frac{\alpha_3 \pm \sqrt{1-\phi^2}}{\alpha_3 - \sqrt{1-\phi^2}} \right]^2 \quad (26a)$$

$$G_{t_{21}} = \frac{\omega_1}{\omega_2} \left[\frac{\alpha_3 \mp \sqrt{1-\phi^2}}{\alpha_3 - \sqrt{1-\phi^2}} \right]^2 \quad (26b)$$

In the positive square root cases, the conversion gains now depend entirely on α_3 , which means physically that variation of the external circuit Q at ω_3 controls conversion gain without changing the input or output admittance at any terminal pair.

The fact that two completely different conversion characteristics arise according to the sign of $\text{Im}(C_1^2 C_2^*)$ is somewhat surprising, since the input and output admittances at all three terminals are independent of this sign. From Figs. 2 and 3 it is evident that the fixed gain cases of Eqs.

25 and 26 must correspond to $W_3 = 0$, which can be verified by solving Eq. 8 for V_3 . With sources first at ω_1 and then at ω_2 , $|V_3|$ is found to vanish independently of γ_3 whenever the negative square roots occur in $G_{t_{12}}$ or $G_{t_{21}}$, respectively. However, in the positive square root cases, $|V_3|$ increases with $G_{t_{12}}$ and $G_{t_{21}}$, for sources at ω_1 and ω_2 , respectively, which is again in agreement with Figs. 2 and 3.

It is interesting to also assume a source at ω_3 and to evaluate the quantities $|V_1 / V_3|$ and $|V_2 / V_3|$. It can be shown that ω_3 couples only to the ω_1 terminals when $G_{t_{12}}$ employs the positive square root, and that ω_3 couples only to the ω_2 terminals with the positive square root in $G_{t_{21}}$. Thus, the sign of $\text{Im}(C_1^2 C_2^*)$ determines the coupling between ω_1 , ω_2 , and ω_3 once the source frequency is specified. In each case, coupling to the external terminals takes place for only two of the three possible frequency pairs. This qualitatively accounts for the two types of up- and down-conversion found in this case.

In summary, for a given magnitude of phase angle between the pump and its harmonic, the results above require the following external circuit adjustments:

$$\text{At } \omega_1: \quad b_1 + \omega_1 C_0 = \varphi; \quad Q_1 = \frac{C_0}{\sqrt{1-\varphi^2}} \left| \frac{C_2}{C_1} \right| \quad (27a)$$

$$\text{At } \omega_2: \quad b_2 + \omega_2 C_0 = \varphi; \quad Q_2 = \frac{C_0}{|C_2| \sqrt{1-\varphi^2}} \quad (27b)$$

$$\text{At } \omega_3: \quad b_3 + \omega_3 C_0 = \varphi; \quad Q_3 < Q_2 \quad (27c)$$

It can be seen from Eqs. 27 that each external terminal will be detuned in the absence of the pump, unless $\varphi = 0$. Also, the necessary external Q 's increase as φ approaches unity. Therefore, the condition $\varphi = 0$ appears to be the preferable operating condition, since it calls for minimum Q circuits and permits circuit tuning prior to the application of the pump signals.

Since the results of this section have led to a small-signal converter with: (1) arbitrary power gain, and (2) conjugately matched input and output terminals, several applications immediately suggest themselves. The first application, which is shown in Fig. 7, is to cascaded up-converters. Here, the gain of each stage can be individually controlled at the respective lower sidebands without requiring any adjustments of the interstage networks. Since each stage of this cascade is an up-converter, it is necessary that $\text{Im}(C_1^2 C_2^*) > 0$ for each stage, which makes the maximum gain in the reverse direction the ratio of input frequency to output frequency. A similar result follows if the sign of $\text{Im}(C_1^2 C_2^*)$ is reversed in each stage, to make the cascade a high gain down-converter.

A modification of this application is shown in Fig. 8, where an up-converter and a down-converter are placed "back-to-back," such that the input and output frequencies are the same. In this configuration the only basic difference between the two stages is in the sign of $\text{Im}(C_1^2 C_2^*)$. Therefore, this circuit yields a nonlinear reactance amplifier with: (1) positive input and output conductance, (2) arbitrary forward gain, and (3) a maximum reverse gain of unity.

It is interesting to apply the Manley-Rowe equations to the circuit in Fig. 8. Since only ω_1 and ω_3 appear at the external terminals,

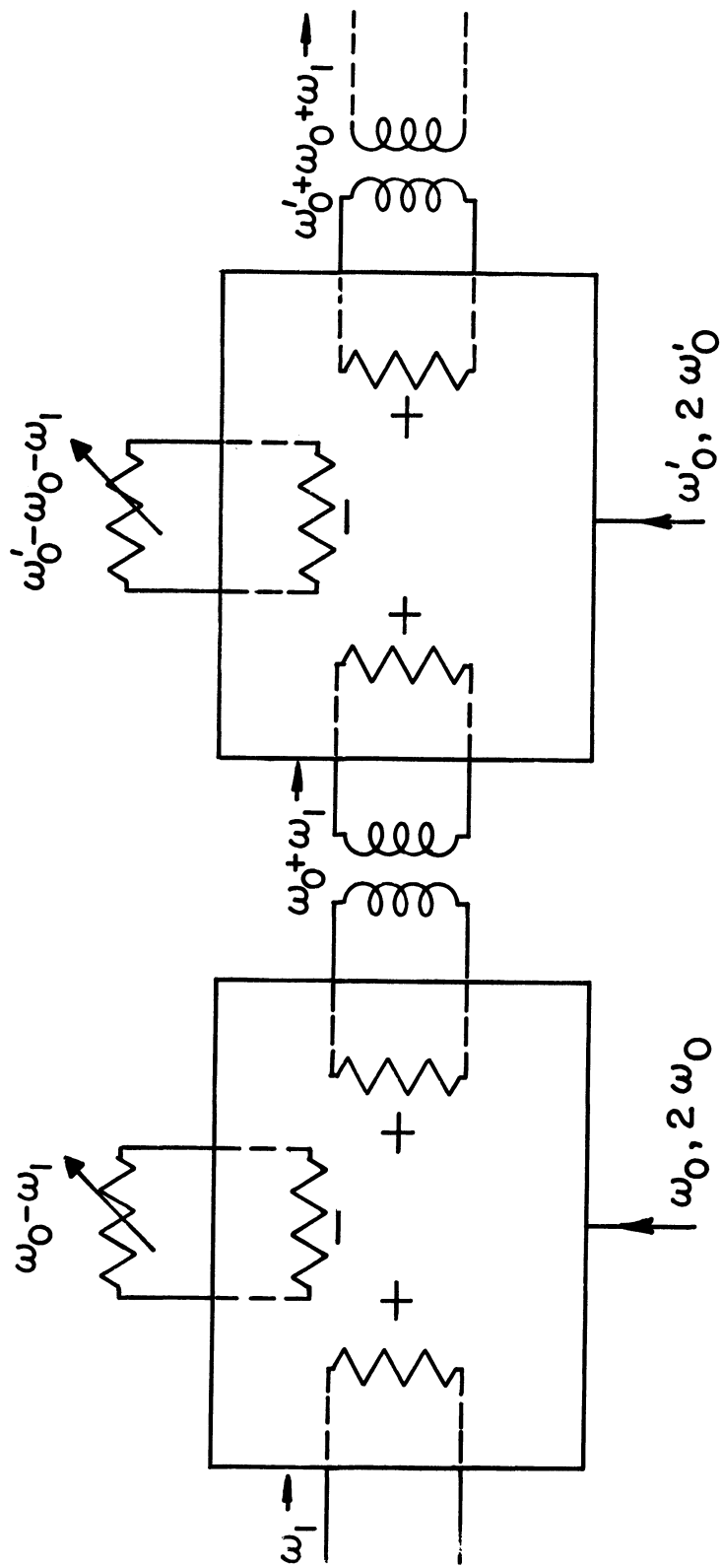


Fig. 7. A cascade of upper-sideband up-converters of the type described in Case 2. The reflected conductances, which are indicated in each box with appropriate signs, are gain-insensitive. Each stage is theoretically capable of unlimited gain.

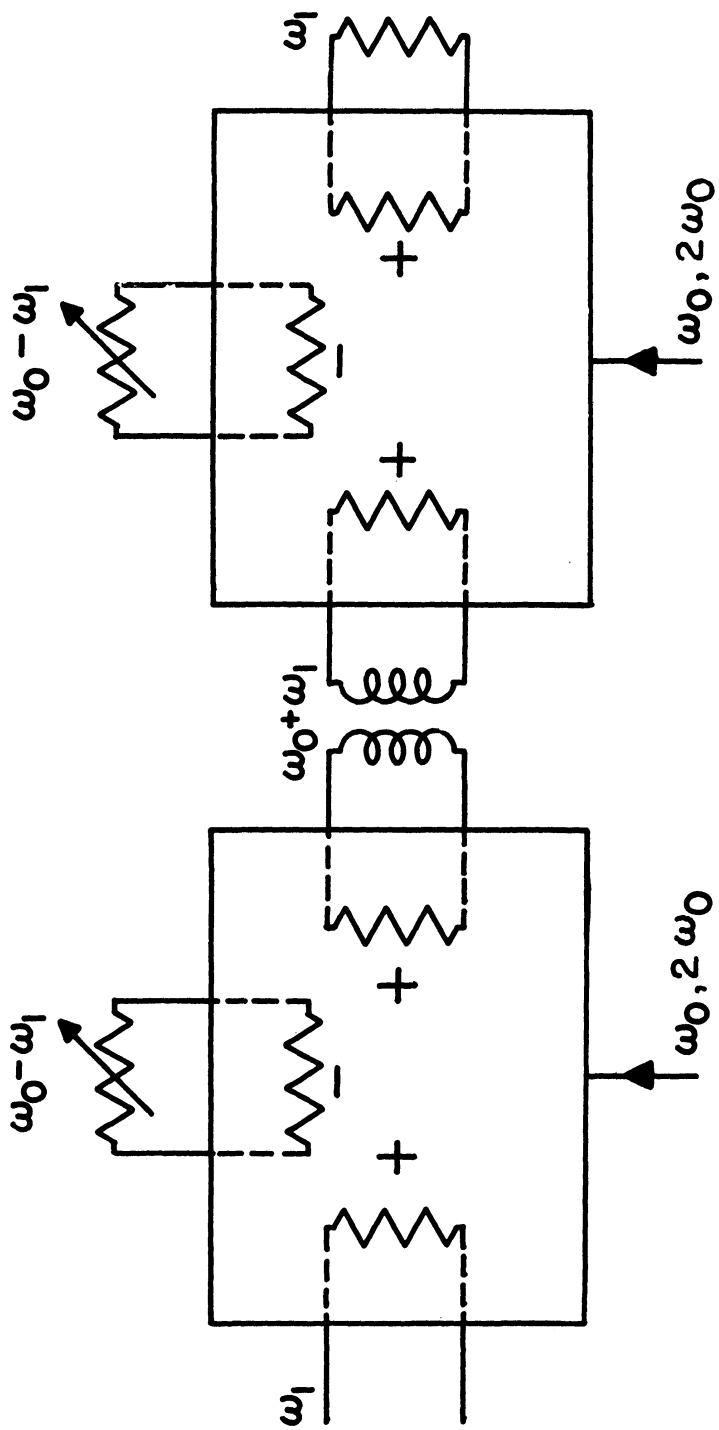


Fig. 8. A positive-input-conductance, nonlinear reactance amplifier formed by cascading an up-converter and a down-converter of the type described in Case 2. The only basic difference between these two stages is in the sign of the phase angle between ω_0 and $2\omega_0$.

this circuit is described by the same special case of Eqs. 1 as is the conventional nonlinear reactance amplifier, where (by Eq. 3b, with $W_2 = 0$)

$$G_{P_{13}} = -\frac{W_3}{W_1} = -\frac{\omega_3}{\omega_1} \quad (28)$$

In this case, however, W_1 has components at two separate terminals and hence can be negative even though the input is conjugately matched.

Although the circuits described above may have desirable gain and control aspects, their noise characteristics will serve as the ultimate test of their value. The primary sources of noise are associated with the external resistances and with internal resistance that is inherently present in any real nonlinear reactance element. In practice, the noise temperature of the output load will generally be fixed and may be large, which is one reason for the use of circulators in conventional negative-input resistance amplifiers and converters. However, with the possibility for conjugate-match offered in this case, output noise that is fed back to the input (due to the semi-directional nature of the circuits under consideration) can be largely absorbed. In addition, the decoupling of sources at ω_3 from the output terminals suggests that the noise contribution of g_3 should be small. Thus, the so-called idler noise that is present in conventional nonlinear reactance circuits should be considerably reduced in this circuit. It can be proposed, therefore, even without the use of circulators, that the noise figure of this circuit should be improved over that of conventional negative-input-resistance amplifiers and converters, even when these latter circuits employ circulators. However, a more precise

estimate of noise figure has not been made at this time, because the original formulation of this problem (i.e., Eq. 7) does not permit the accurate inclusion of losses internal to the nonlinear reactance element.

4. CONCLUSION

A detailed analysis of Eq. 8, or equivalently, Fig. 4, has demonstrated several useful extensions of conventional nonlinear reactance circuits. It has been shown that parametric amplification at a frequency higher than the pump can, from the point of view of the nonlinear reactance element, be the same order of effect as conventional parametric amplification at a frequency lower than the pump. Also, a nonlinear reactance circuit has been developed that is capable of unlimited up- or down-conversion gain without reflecting negative resistance at either the input or output terminals. The latter result suggests a means by which a nonlinear reactance amplifier can be obtained which does not require a circulator for optimum performance. A more detailed summary of the results of this analysis is given in Table I. Within the limits of approximation provided by the circuit model in Fig. 4, Table I contains a compilation of the more important conclusions regarding three- and four-frequency, nonlinear reactance circuits.¹

1. The term "four-frequency" has been employed throughout this paper even though a fifth frequency, in the form of the pump harmonic, has frequently been included. This choice of nomenclature has been made because only one of the two pump components need be applied externally and hence only four frequencies need be observed at external terminals.

TABLE I

A SUMMARY OF THE MAJOR EFFECTS OBTAINABLE FROM THE NONLINEAR REACTANCE CIRCUIT MODEL OF FIG. 4.

In entries where one or more frequencies or time-varying capacity components are omitted, they are assumed to be short circuited.

Key: C.G. = conversion gain; P.A. = gain by parametric amplification; I.R. = input resistance; and T = tuning conditions.

Frequencies	Pump Components		
	(a) C_1 only	(b) C_2 only	(c) C_1 and C_2
(1) ω_1, ω_2	C.G.: Limited P.A.: None I.R.: Positive T: Gain independent	No effects	Same as (1a)
(2) ω_1, ω_3	C.G.: Unlimited P.A.: Unlimited I.R.: Negative T: Gain independent	No effects	Same as (2a)
(3) ω_2, ω_3	No effects	Same as (2a)	Same as (2a)
(4) $\omega_1, \omega_2, \omega_3$	C.G.: Unlimited P.A.: Unlimited I.R.: Positive T: -Gain dependent -Tuning impossible at all three frequencies	Same as (3b)	C.G.: Unlimited P.A.: Unlimited I.R.: -Positive at ω_1 and ω_2 -Negative at ω_3 T: Gain independent

APPENDIX

Proofs of Theorems 1 and 2 can be obtained from Eqs. 15 by the following considerations. Recalling that $\gamma_{K_{IN}} = \alpha_{K_{IN}} + j\beta_{K_{IN}}$ ($K = 1, 2, 3$), the conditions for resonance at each pair of terminals in Fig. 4 (with $|C_2| = 0$) become

$$\text{at } \omega_1: \quad \beta_{1_{IN}} = \beta_1 + \frac{\beta_3}{|\gamma_3|^2} - \frac{\beta_2}{|\gamma_2|^2} = 0 \quad (29a)$$

$$\text{at } \omega_2: \quad \beta_{2_{IN}} = \beta_2 - \frac{\beta_3 + \beta_1|\gamma_3|^2}{|\gamma_1\gamma_3 - 1|^2} = 0 \quad (29b)$$

$$\text{at } \omega_3: \quad \beta_{3_{IN}} = \beta_3 - \frac{\beta_2 - \beta_1|\gamma_2|^2}{|\gamma_1\gamma_2 + 1|^2} = 0 \quad (29c)$$

Similarly, the conditions for circuit stability are

$$\text{at } \omega_1: \quad \alpha_{1_{IN}} = \alpha_1 + \frac{\alpha_2}{|\gamma_2|^2} - \frac{\alpha_3}{|\gamma_3|^2} > 0 \quad (30a)$$

$$\text{at } \omega_2: \quad \alpha_{2_{IN}} = \alpha_2 + \frac{\alpha_1|\gamma_3|^2 - \alpha_3}{|\gamma_1\gamma_3 - 1|^2} > 0 \quad (30b)$$

$$\text{at } \omega_3: \quad \alpha_{3_{IN}} = \alpha_3 - \frac{\alpha_2 + \alpha_1|\gamma_2|^2}{|\gamma_1\gamma_2 + 1|^2} > 0 \quad (30c)$$

Therefore, Eqs. 30 are explicit expressions for the basic conditions under which Theorems 1 and 2 apply.

The proof of Theorems 1 and 2 will now be divided into the following steps:

Step A. It is easily seen that there are two possible conditions under which Eqs. 29a and 29c can be satisfied simultaneously; namely,

$$\beta_3 = 0 \quad (31a)$$

or

$$\left| \frac{\gamma_3}{\gamma_2} \right|^2 = \frac{1}{|\gamma_1 \gamma_2 + 1|^2} \quad (31b)$$

However, for Eqs. 30a and 30c to be satisfied simultaneously it is necessary that

$$\frac{1}{|\gamma_1 \gamma_2 + 1|^2} < \frac{\alpha_3}{\alpha_2 + \alpha_1 |\gamma_2|^2} < \left| \frac{\gamma_3}{\gamma_2} \right|^2 \quad (32)$$

Therefore, of the two possible conditions described in Eqs. 31, only Eq. 31a will yield both stability and resonance at ω_1 and ω_3 .

Step B. If $\beta_3 = 0$, the condition for resonance at ω_1 and ω_3 becomes $\beta_1 |\gamma_2|^2 = \beta_2$, which, with the aid of Eq. 29b, reduces Eq. 30b to the following expression

$$\alpha_{2_{IN}} = \alpha_2 \pm \alpha_2 \left(1 + \frac{\beta_2 \beta_{2_{IN}}}{\alpha_2^2} \right)^{\frac{1}{2}} \left(1 - \frac{\beta_{2_{IN}}}{\beta_2} \right)^{\frac{1}{2}} > 0 \quad (33)$$

However, for parametric amplification at ω_2 , Eq. 33 must be satisfied in such a way that the second term takes on the negative sign. Clearly, this is not possible if $\beta_{2_{IN}} = 0$. Consequently, if $\beta_{1_{IN}} = \beta_{3_{IN}} = 0$, then $\beta_{2_{IN}} \neq 0$ is necessary for parametric amplification at ω_2 . $\beta_{2_{IN}} = 0$ can occur only if $\alpha_{2_{IN}}$ equals $2\alpha_2$ or zero (i.e., only under conditions of

conjugate match or infinite gain at ω_2).

Step C. This step amounts simply to recalling that, under Case 1b of the text, $\beta_{2_{IN}} = 0$ and $\beta_3 = 0$ were shown to yield $\beta_{1_{IN}} \neq 0$ and $\beta_{3_{IN}} \neq 0$ in the region of parametric amplification at ω_2 .

Therefore, under the conditions stated in Theorem 1, $\beta_3 = 0$ yields either $\beta_{1_{IN}} = \beta_{3_{IN}} = 0$ and $\beta_{2_{IN}} \neq 0$ (step B), or $\beta_{2_{IN}} = 0$, $\beta_{1_{IN}} \neq 0$, and $\beta_{3_{IN}} \neq 0$ (step C). Similarly, with $\beta_3 \neq 0$, $\beta_{1_{IN}}$ and $\beta_{3_{IN}}$ cannot vanish simultaneously (step A). Therefore, stable parametric amplification at ω_2 , with $|C_2| = 0$, requires at least one of the three quantities, $\beta_{1_{IN}}$, $\beta_{2_{IN}}$, or $\beta_{3_{IN}}$, to not vanish, which proves Theorem 1.

Now consider Theorem 2. By steps A and B above, the necessary and sufficient conditions for ω_1 and ω_3 to be both resonant and stable (see Footnote p. 20) are

$$\beta_3 = 0 \quad (34a)$$

$$\beta_2 = \beta_1 |\gamma_2|^2 \quad (34b)$$

$$\alpha_1 - \frac{1}{\alpha_3} > \frac{-\alpha_2}{|\gamma_2|^2} \quad (34c)$$

If Eqs. 34 are satisfied, Eq. 30b yields

$$\alpha_1 - \frac{1}{\alpha_3} > \frac{-1}{2\alpha_2} \cdot \left[1 - (1 - 4\alpha_2^2 \beta_1^2) \right]^{\frac{1}{2}} \quad (35)$$

to be necessary and sufficient for stability at ω_2 . However, by Eq. 34b

$$1 - 4\alpha_2^2 \beta_1^2 = \left[\frac{\alpha_2^2 - \beta_2^2}{\alpha_2^2 + \beta_2^2} \right]^2 \quad (36)$$

whereupon Eq. 35 yields

$$\alpha_1 - \frac{1}{\alpha_3} > -\frac{\alpha_2}{|\gamma_2|^2} \left[\text{lesser of } \left(1, \frac{\beta_2^2}{\alpha_2} \right) \right] \quad (37)$$

as the necessary and sufficient condition for stability at ω_2 . Since Eq. 37 is also sufficient for stability at ω_1 and ω_3 , the proof of Theorem 2 is completed.

REFERENCES

1. J. M. Manley and H. E. Rowe, "Some General Properties of Nonlinear Elements - Part I. General Energy Relations," Proc. IRE, Vol. 44, pp. 904-913, July 1956.
2. C. L. Hogan, R. L. Jepsen, and P. H. Vartanian, "New Type of Ferromagnetic Amplifier," J. Appl. Phys., Vol. 29, pp. 422-423, March 1958.
3. S. Bloom and K. K. N. Chang, "Parametric Amplification Using Low Frequency Pumping," Proc. IRE, Vol. 46, pp. 1383 - 1387, July 1958.
4. H. E. Rowe, "Some General Properties of Nonlinear Elements - Part II. Small Signal Theory," Proc. IRE, Vol. 46, No. 5, May 1958, pp. 850-860.
5. D. Lennox, "Gain and Noise Figure of a Variable Capacitance Up-Converter," Bell Sys. Tech. J., Vol. 37, pp. 989-1008, July 1958.

DISTRIBUTION LIST

2 Cys	Commanding Officer U.S. Army Signal Research and Development Laboratory Fort Monmouth, New Jersey ATTN: Senior Scientist Counter- measures Division	2 Cys	Commander, Wright Air Development Center Wright-Patterson Air Force Base, Ohio ATTN: WCOSI-3
1 Cy	Commanding General U.S. Army Electronic Proving Ground Fort Huachuca, Arizona ATTN: Director, Electronic Warfare Department	1 Cy	Commander, Wright Air Development Center Wright-Patterson Air Force Base, Ohio ATTN: WCLGL-7
1 Cy	Chief, Research and Development Divi- sion, Office of the Chief Signal Officer Department of the Army Washington 25, D.C. ATTN: SIGEB	1 Cy	Commander, Air Force Cambridge Research Center L.G. Hanscom Field Bedford, Massachusetts ATTN: CROTLR-2
1 Cy	Chief, Plans and Operations Division Office of the Chief Signal Officer Washington 25, D.C. ATTN: SIGEW	1 Cy	Commander, Rome Air Development Center Griffiss Air Force Base, New York ATTN: RCSSLD
1 Cy	Commanding Officer Signal Corps Electronics Research Unit 9560th USASRU, P.O. Box 205 Mountain View, California	1 Cy	Commander, Air Proving Ground Center ATTN: Adj/Technical Report Branch Eglin Air Force Base, Florida
1 Cy	U.S. Atomic Energy Commission 1901 Constitution Avenue, N.W. Washington 25, D.C. ATTN: Chief Librarian	1 Cy	Commander, Special Weapons Center Kirtland Air Force Base Albuquerque, New Mexico
1 Cy	Director, Central Intelligence Agency 2430 E Street, N.W. Washington 25, D.C. ATTN: OCD	1 Cy	Chief, Bureau of Ordnance Code ReO-1, Department of the Navy Washington 25, D.C.
1 Cy	Signal Corps Liaison Officer Lincoln Laboratory Box 73 Lexington 73, Massachusetts ATTN: Col. Clinton W. Janes	1 Cy	Chief of Naval Operations, EW Systems Branch, OP-347, Department of the Navy Washington 25, D.C.
10 Cys	Commander, Armed Services Technical Information Agency Arlington Hall Station Arlington 12, Virginia	1 Cy	Chief, Bureau of Ships, Code 840 Department of the Navy Washington 25, D.C.
1 Cy	Commander, Air Research & Development Command Andrews Air Force Base Washington 25, D.C. ATTN: RDTC	1 Cy	Chief, Bureau of Ships, Code 843 Department of the Navy Washington 25, D.C.
1 Cy	Directorate of Research & Development USAF Washington 25, D.C. ATTN: Chief, Electronic Division	1 Cy	Chief, Bureau of Aeronautics Code EL-8, Department of the Navy Washington 25, D.C.
		1 Cy	Commander, Naval Ordnance Test Station Inyokern, China Lake, California ATTN: Test Director-Code 30
		1 Cy	Commander, Naval Air Missile Test Center Point Mugu, California ATTN: Code 366

DISTRIBUTION LIST (Cont'd)

1 Cy	Commanding Officer U.S. Naval Ordnance Laboratory Silver Spring 19, Maryland	1 Cy	Stanford Electronics Laboratories Stanford University Stanford, California ATTN: Applied Electronics Laboratory Document Library
2 Cys	Chief, U.S. Army Security Agency Arlington Hall Station Arlington 12, Virginia ATTN: GAS-24L	1 Cy	HRB-Singer, Inc. Science Park State College, Penna. ATTN: R. A. Evans, Manager, Technical Information Center
1 Cy	President, U.S. Army Defense Board Headquarters Fort Bliss, Texas	1 Cy	ITT Laboratories 500 Washington Avenue Nutley 10, New Jersey ATTN: Mr. L. A. DeRosa, Div. R-15 Lab.
1 Cy	President, U.S. Army Airborne and Electronics Board Fort Bragg, North Carolina	1 Cy	The Rand Corporation 1700 Main Street Santa Monica, California ATTN: Dr. J. L. Hult
1 Cy	U.S. Army Antiaircraft Artillery and Guided Missile School Fort Bliss, Texas ATTN: E&E Dept.	1 Cy	Stanford Electronics Laboratories Stanford University Stanford, California ATTN: Dr. R. C. Cumming
1 Cy	Commander, USAF Security Service San Antonio, Texas ATTN: CLR	1 Cy	Willow Run Laboratories The University of Michigan P. O. Box 2008 Ann Arbor, Michigan ATTN: Dr. Boyd
1 Cy	Chief of Naval Research Department of the Navy Washington 25, D.C. ATTN: Code 931	1 Cy	Stanford Research Institute Menlo Park, California ATTN: Dr. Cohn
1 Cy	Commanding Officer U.S. Army Security Agency Operations Center Fort Huachuca, Arizona	2 Cys	Commanding Officer, U.S. Army Signal Missile Support Agency White Sands Missile Range, New Mexico ATTN: SIGWS-EW and SIGWS-FC
1 Cy	President, U.S. Army Security Agency Board Arlington Hall Station Arlington 12, Virginia	1 Cy	Commanding Officer, U.S. Naval Air Development Center Johnsville, Pennsylvania ATTN: Naval Air Development Center Library
1 Cy	Operations Research Office Johns Hopkins University 6935 Arlington Road Bethesda 14, Maryland ATTN: U.S. Army Liaison Officer	1 Cy	Commanding Officer, U.S. Army Signal Research & Development Laboratory Fort Monmouth, New Jersey ATTN: U.S. Marine Corps Liaison Office, Code AO-4C
1 Cy	The Johns Hopkins University Radiation Laboratory 1315 St. Paul Street Baltimore 2, Maryland ATTN: Librarian		

DISTRIBUTION LIST (Cont'd)

1 Cy	Commanding Officer, U.S. Army Signal Research & Development Laboratory Fort Monmouth, New Jersey ATTN: ARDC Liaison Office	1 Cy	Director, National Security Agency Ft. George G. Meade, Maryland ATTN: TEC
1 Cy	President, U.S. Army Signal Board Fort Monmouth, New Jersey	1 Cy	Dr. H. W. Farris, Director, Electronic Defense Group, University of Michigan Research Institute Ann Arbor, Michigan
11 Cys	Commanding Officer, U.S. Army Signal Research & Development Laboratory Fort Monmouth, New Jersey ATTN: 1 Cy - Director of Research 1 Cy - Technical Documents Center - ADT/E 1 Cy - Chief, Ctms Systems Branch, Countermeasures Division 1 Cy - Chief, Detection & Location Branch, Countermeasures Div. 1 Cy - Chief, Jamming & Deception Branch, Countermeasures Div. 1 Cy - File Unit No. 4, Mail & Records, Countermeasures Div. 1 Cy - Chief, Vulnerability Br, Electromagnetic Environment Div. 1 Cy - Reports Distribution Unit, Countermeasures Div. File 3 Cys- Chief, Security Division (for retransmittal to BJSM)	20 Cys	Electronic Defense Group Project File University of Michigan Research Institute Ann Arbor, Michigan
		1 Cy	Project File University of Michigan Research Institute Ann Arbor, Michigan
		1 Cy	Director, Air University Library Maxwell Air Force Base, Alabama ATTN: CR-4987
		1 Cy	Commanding Officer-Director U.S. Naval Electronic Laboratory San Diego 52, California
		1 Cy	Office of the Chief of Ordnance Department of the Army Washington 25, D.C. ATTN: ORDTU
		1 Cy	Chief, West Coast Office U.S. Army Signal Research and Development Laboratory Bldg. 6 75 S. Grand Avenue Pasadena 2, California
1 Cy	Director, Naval Research Laboratory Countermeasures Branch, Code 5430 Washington 25, D.C.		
1 Cy	Director, Naval Research Laboratory Washington 25, D.C. ATTN: Code 2021		

Above distribution is effected by Countermeasures Division, Surveillance Dept., USASRDL, Evans Area, Belmar, New Jersey. For further information contact Mr. I. O. Myers, Senior Scientist, telephone PROspect 5-3000, Ext. 61252.

UNIVERSITY OF MICHIGAN



3 9015 02493 1068